Journal of Sustainable Development of Energy, Water and Environment Systems

http://www.sdewes.org/jsdewes

Year 2020, Volume 8, Issue 3, pp 561-576

Numerical Investigation of Inner Blade Effects on the Conventional Savonius Rotor with External Overlap

Mohanad Al-Ghriybah*[1], Mohd F. Zulkafli[2], Djamal H. Didane[3]

[1]Department of Aeronautical Engineering, Faculty of Mechanical and Manufacturing Engineering, Universiti Tun Hussein Onn Malaysia, 86400 Parit Raja, Johor, Malaysia
Department of Renewable Energy Engineering, Faculty of Engineering, Al-Isra University, Al Hezam Road, Amman, Jordan
e-mail: Mohanad.alghriybah@gmail.com

[2]Department of Aeronautical Engineering, Faculty of Mechanical and Manufacturing Engineering, Universiti Tun Hussein Onn Malaysia, 86400 Parit Raja, Johor, Malaysia
e-mail: fadhli@uthm.edu.my

[3]Department of Energy and Thermofluid Engineering, Faculty of Mechanical and Manufacturing Engineering, Universiti Tun Hussein Onn Malaysia, 86400 Parit Raja, Johor, Malaysia
e-mail: djamal@uthm.edu.my

Cite as: Al-Ghriybah, M., Zulkafli, M. F., Didane, D. H., Numerical Investigation of Inner Blade Effects on the Conventional Savonius Rotor with External Overlap, J. sustain. dev. energy water environ. syst., 8(3), pp 561-576, 2020, DOI: https://doi.org/10.13044/j.sdewes.d7.0292

ABSTRACT

The Savonius wind turbine is considered as one of the best vertical axis wind turbines for harvesting the kinetic energy from the wind in the urban areas, due to magnificent features such as high starting torque, low construction and maintenance costs, simple design, and self-starting ability especially at low wind speed. However, the conventional style of the Savonius rotor suffers from low efficiency. Consequently, modifying the configuration of the rotor may be an appropriate solution for providing electricity to the communities with no access to the power grid. Thus, this study aims to enhance the performance of the conventional Savonius rotor with an external overlap by adding an inner blade to the rotor configuration. Hence, a comparison study between five new arrangements against the conventional rotor in terms of power coefficient (C_p) and torque coefficient (C_t) is performed through a two-dimensional simulation by using ANSYS Fluent 19.2. The k-ε/Realizable turbulence model is employed in the simulation. Results conclude that inner blade with an angle of 120° increases the power coefficient by 41%, 39%, and 7% at tip speed ratio (TSR) = 0.7, 0.6, and 0.5, respectively.

KEYWORDS

Savonius, Vertical-axis wind turbines, Inner blade, External overlap, Wind energy, S-rotor.

INTRODUCTION

The rapid energy consumption, population growth, consumption of traditional energy sources, and the environmental issues are pushing most of the world countries to the efficient use of clean and renewable energy sources. In recent years, electricity production from renewable sources has been increased as being clean and available [1]. Amongst the renewable sources, wind energy has turned into a favourite source of

* Corresponding author

renewable energy due to the technological features and low cost of the generated electricity [2]. In general, two main arrangings of wind machines subsist: Vertical turbines, whereby the turbine blades rotate on a perpendicular axis to the wind direction (VAWT) and the horizontal turbines, whereby the blades spin on an axis with the same direction of the wind (HAWT). HAWT has higher efficiency compared to the VAWT, so it is very common in the large-scale systems which require high amounts of electricity [3]. Recently, VAWTs have become more popular in many countries, especially in small-scale systems. In spite of their low efficiency, they have several features over the HAWTs such as low noise, less cost, simple in construction, independent wind directions and ease of maintenance whereby the generator is placed on the ground [4]. Savonius and Darrieus wind rotors are considered as the main configurations in the VAWTs family [5]. Darrieus rotor overcomes Savonius rotor with higher efficiency, in the same time, Savonius rotor has many features over the Darrieus rotor such as the ability to self-start, high starting torque, low maintenance costs, and less noise [6, 7]. These features make the Savonius rotor attractive for researchers in order to develop and increase its efficiency. Savonius rotor has a strong structural design, the whole turbine system can be built-up and installed near to the ground level. Typically it comprises of two semi-cylindrical buckets with a distinctive overlap between them, and end plates which attached at the top and bottom of the rotor as shown in Figure 1.

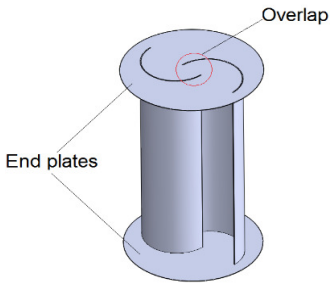

Figure 1. Savonius wind rotor with internal overlap and end plates

Due to the main feature of the Savonius rotor, self-starting, studies have been conducted on the Savonius rotor as a starter for the other types of the VAWTs which suffered from low starting performance. Sahim *et al*. [8] have suggested the combine between Savonius and Darrieus rotors which will give better performance at low wind speeds. Torque coefficient (C_t) was evaluated for various Tip Speed Ratio (*TSR*) with different values of turbine diameter. A hybrid Savonius-Darrieus wind turbine to improve the starting performance was performed by Liang *et al*. [9]. Enhancement for the torque coefficient, power coefficient (C_p), and self-starting capability at different radius ratio and attachment angles for different *TSR* was reached. In the same way, ed-Dîn Fertahi *et al*. [10] performed a study on the Savonius-Darrieus hybrid wind turbine to estimate the effect of blade's angular position on the self-start ability over various ranges of *TSR*. An integration of a Savonius rotor and H-rotor in order to make the system completely self-starting and enhance the power performance was carried out by Bhuyan and Biswas [11]. Ghosh *et al*. [12] performed a three-dimensional simulation using Computational Fluid Dynamic (CFD) model in order to study the aerodynamics of the three-bladed Darrieus Savonius rotor. Authors conclude that such a hybrid system is recommended for wind power conversion due to the improvement in the performance at low wind speeds.

Overall the literature, the main negative of the Savonius rotor was the low efficiency, this is mainly due to the negative torque which generates on the returning blade with the convex side [13, 14]. Many aerodynamic improvements have been accomplished on Savonius wind turbine in recent decades by researchers as the performance of the traditional turbine is low [15].

Influence of different parameters on the efficiency of Savonius wind turbine was investigated in the previous studies such as number of stages, overlap ratio, aspect ratio, number of blades, and use of accessories such as end plates and power augmentation devices. Two-stage Savonius turbine performs better than the single-stage turbine in terms of static torque [16]. Low values of overlap ratio enhance the performance of the Savonius rotor as reported in many studies [17, 18]. Using high values of aspect ratio is recommended to increase the angular velocity of the rotor and so improve the coefficient of power [19, 20]. Three bladed rotors reduce the performance compares to the two-bladed rotors [21, 22]. The extracted power from the Savonius rotor can be improved by preventing air leakage from the concave side to the external airflow by using end plates [23]. The performance of the Savonius rotor can be improved by utilizing power augmentation devices such as deflector plates and windshields. Deflector plates are placed in front of the returning blades in order to reduce wind resistance [24]. Moreover, they enhance the self-starting capability with a net positive static torque [25]. However, although the Savonius rotor was invented in 1922, the research related to this turbine is still of a genuine interest in the last decade. The current increasing research on the vertical turbines could mainly be imputed to the recent discoveries that small-scale vertical turbines could be more appropriate and operate more effectively in low wind speed regions [26]. Given that it offers sundry features over its counterpart horizontal turbine in terms of capability to perform very well in highly turbulent and low wind speed regions. Additionally, the noise caused by the rotation of blades is low due to the lower spinning speed and the simple design [27].

While there are various effective techniques to harvest wind energy, many researchers are trying to enhance the performance of the Savonius rotor in terms of C_p by optimizing the shape of blades or adding power augmentations like wind deflectors.

The design of the Savonius rotor needs to be the focuses of development in order to enhance the generated torque by the wind rotor. Thus, there should be research on the Savonius rotor in relation to the addition of inner blade in order to enhance the performance of the turbine. Therefore, in this study, a new blade configuration of Savonius rotor having an inner blade with external overlap is proposed. One of the advantages of this new configuration is more energy could be captured from the wind compared to the conventional Savonius rotor. The study has been conducted with the assist of numerical simulations performed using ANSYS Fluent. The study has been conducted with the assist of numerical simulations performed using ANSYS Fluent.

TURBULENCE MODEL

The realizable *k-ε* turbulence model was employed in the simulation which has two equations [28]. The main features of this model include enhanced performance inflow with recirculation and a strong pressure gradient. The transport equation for k and ε in the model are given as Mohamed *et al.* [29]:

$$\frac{\partial}{\partial t}(\rho k)+\frac{\partial}{\partial x_j}(\rho k u_j)=\frac{\partial}{\partial x_j}\left[\left(\mu+\frac{\mu_t}{\sigma_k}\right)\frac{\partial k}{\partial x_j}\right]+G_k+G_b-\rho\varepsilon-Y_M+S_k \quad (1)$$

$$\frac{\partial}{\partial t}(\rho \varepsilon)+\frac{\partial}{\partial x_j}(\rho \varepsilon u_j)=\frac{\partial}{\partial x_j}\left[\left(\mu+\frac{\mu_t}{\sigma_\varepsilon}\right)\frac{\partial \varepsilon}{\partial x_j}\right]+\rho C_1 S_\varepsilon-\rho C_2\frac{\varepsilon^2}{k+\sqrt{\nu\varepsilon}}+C_{1\varepsilon}\frac{\varepsilon}{k}C_3 G_b+S_\varepsilon \quad (2)$$

where μ_t is the eddy viscosity, σ_k and σ_ε are diffusion constants of the model, $C_1=\max\left[0.43,\frac{\eta}{\eta+5}\right],\eta=S\frac{k}{\varepsilon},S=\sqrt{2S_{ij}S_{ij}}$, G_k and G_b are the generation of turbulent kinetic energy due to the mean velocity gradient and the buoyancy, respectively, Y_M is the contribution of the fluctuating dilatation in compressible turbulence to the overall

dissipation rate, and S_k and S_ε are the user-defined functions. The employed values of constants in the computations are shown in Table 1.

Table 1. Turbulence model constants

Constant	$C_{1\varepsilon}$	C_2	σ_k	σ_ε
Value	1.44	1.90	1.00	1.20

NUMERICAL METHODS

ANSYS is a CFD software for analyzing simple and complex geometries, steady and transient problems. It can predict the aerodynamics of wind turbines whether in two-dimensions or in three-dimensions whereby the analysis starts by generating the CAD geometry and end up with post-processing of the results.

For the present study, a two-dimensional simulation was adopted utilizing ANSYS Fluent 19.2 software. Fluid flow around turbine geometries can be solved in efficient and realistic simulation using Fluent whereby the generated result can give a comprehensive study without any costs [30]. Consequently, a transient 2D simulation was selected in ANSYS Fluent 19.2 to obtain a steady solution from the initial boundary conditions.

Geometry configuration

A comparison study between the conventional Savonius rotor with an external overlap of e = 0.02 m against the novel configuration of the rotor was carried out. In Figure 2 and Figure 3, a top view of the conventional and novel configurations rotors are shown, and their detailed dimensions are listed in Table 2. The conventional blade was taken with a fixed diameter of d = 0.188 m. The diameter of the inner blade was d_i = 0.144 m. In addition, the inner blade arc angle was changed between the values (180-100) by a step of 20 degrees in each time. Abraham *et al*. [31] have reported that the end plates increase the performance of the Savonius rotor. Additionally, authors like Plourde *et al*. [32] and Fujisawa and Gotoh [33] have assured as optimum an end plates diameter of D_e = 1.1D to enhance the rotor performance. Consequently, end plates, D_e = 0.4862 m was taken for all tested turbines. The shaft diameter was taken 0.03 m.

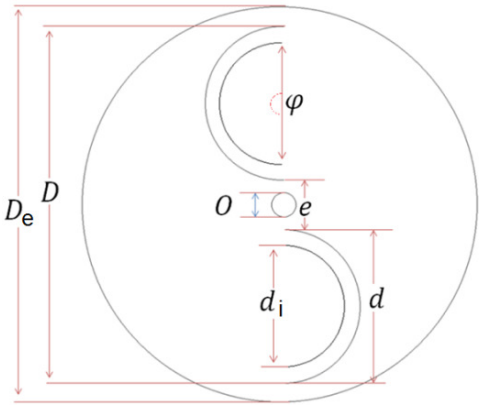

Figure 2. Main proposed configuration with external overlap

Previous studies showed a lack of consensus about the optimum value of overlap ratio. Savonius rotor with an internal overlap ratio between their blades shows a better performance in their starting [15]. On the other hand, studies such as Driss *et al*. [34] have determined that the external overlap between the blades decreases the performance of the conventional rotor. Thus, the current study aims to increase the performance of the rotor with an external overlap.

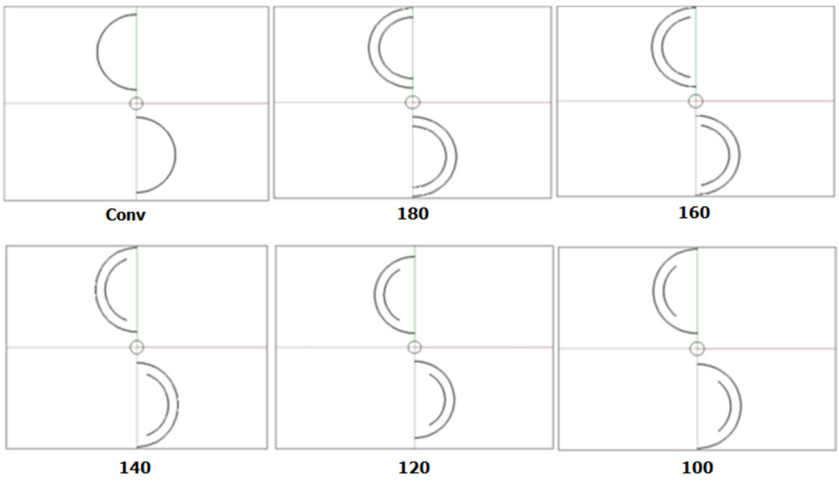

Figure 3. Proposed configurations

Table 2. Rotors dimension

Geometry	φ inner blade	d_i [m]	Arc length of inner blade [m]	D [m]	D_e [m]	d [m]	e [m]	O [m]
Conventional blade	-	-	-	0.442	0.4862	0.188	0.02	0.03
Main configuration	180°	0.144	0.2262	0.442	0.4862	0.188	0.02	0.03
Model 1	160°	0.144	0.2010	0.442	0.4862	0.188	0.02	0.03
Model 2	140°	0.144	0.1759	0.442	0.4862	0.188	0.02	0.03
Model 3	120°	0.144	0.1508	0.442	0.4862	0.188	0.02	0.03
Model 4	100°	0.144	0.1256	0.442	0.4862	0.188	0.02	0.03

Computational domain and boundary conditions

It is necessary to mention that the two-dimensional simulation can predict the performance of the rotor with high accuracy [35]. Moreover, the cross-section of the rotor is the same along it height which means that we can neglect the flow in the vertical axis which is also equivalent to the three-dimension simulation for the rotors with end plates [36, 37]. Consequently, since this study focuses more on some key modeling details rather than waiting for three-dimension complex geometries to be solved, a two-dimensional modeling is selected.

In order to build a suitable computational domain for a wind turbine modelling, two conditions must be followed: firstly, the dimensions have to be large enough in a way that the domain walls have no effect on the airfield and secondly, the domain must not be extremely large in order to reach the optimal solution by using the computational resources in an effective way. The simulation domain, mainly, consists of two sub-domains: a moving domain and a stationary domain. The moving domain is where the rotor will start moving in a certain rotational speed, whereas, the stationary domain contains the flowing air and represents the wind tunnel. Therefore, the dimensions of the simulation domain must be extended at least 10 times the rotor diameter to avoid the influence of the boundary conditions on the results [38].

The computational domain utilized in this study is shown in Figure 4. The circular region with moving mesh has a dimension of 1.1D. The center of the shaft is placed at a distance of 5D from both upper and lower sides. These two subdomains are parted by a defined interface. At the inlet, a constant wind speed U of 9 m/s was used. The outlet of the domain was set as a pressure outlet. Stationary walls at the top and bottom of the domain and blade wall are set to no-slip condition. Rotor angular speed is set to five degrees/step to minimize the simulation time. The air stream was turbulent flow with 2.69×10^5 Reynolds number (Re).

Pressure-based transition simulation is used in the general setting of fluent solver. For pressure-velocity coupling, the SIMPLE algorithm is adopted since the solver was set to

a transient pressure-based. The spatial discretization of the conservative equations is treated with a second-order upwind scheme.

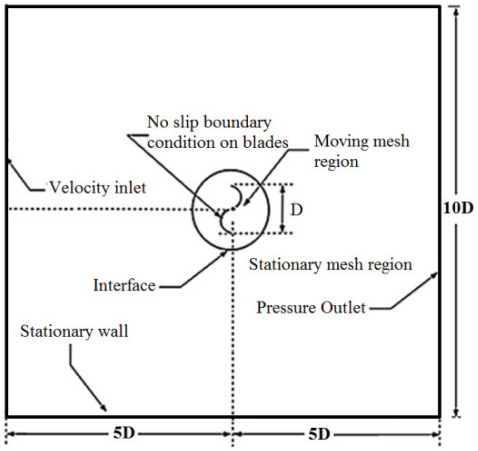

Figure 4. Schematic diagram of the computational domain

Meshing considerations

The moving sub-domain was meshed using unstructured mesh whereas a refinement was applied to the interface between the two sub-domains to enhance the adaptation of the rotor geometry. The boundary layer effect can be defined in the ANSYS software as the inflation on the rotor blades which take into consideration the energy loss due to the friction. In addition to the fine mesh around the blades, y^+ factor should be taken into consideration, this factor estimates the thickness of the first inflation layer. According to Yu and Thé [39], y^+ represents the proportion between turbulent and laminar effects in a cell. The desirable value of y^+ factor is around 1 [40], this value gives more accurate solution nearby the boundary layer. The non-dimensional factor can be calculated using the following equation:

$$y^+ = \frac{\rho U_t y}{\mu} \tag{3}$$

where ρ [kg/m^3] is the air density, U_t [m/s] is the friction velocity, y is the thickness of the first boundary layer on the blades and μ [kg/ms] is the dynamic viscosity.

The friction velocity can be obtained using the following equation:

$$U_t = \sqrt{\frac{\tau_w}{\rho}} = U\sqrt{\frac{C_f'}{2}} \tag{4}$$

where τ_w represents the wall shear stress and C_f' represents the coefficient of friction. The approximated coefficient of friction can be calculated as follows [5]:

$$\frac{C_f'}{2} \approx \frac{0.037}{\mathrm{Re}_L^{1/5}} \tag{5}$$

In the beginning, a mesh convergence test was carried out through various grids in order to make the solution independent of the grid size. Coarse, medium and fine meshes were generated using mechanical mesh in ANSYS software. To validate the mesh selection, a model proposed by Hayashi *et al*. [41] was created and simulated, grid sizes

were taken as listed in Table 3. To assure the convergence of the solution, the solver time step was set to cover ten full rotations. Validation results are illustrated in Figure 5. The average percentage of error is less than 7% for both medium and fine mesh when it compared to the experimental results of Hayashi *et al.* [41]. The medium grid was adopted for this study in order to reduce the simulation time. Including the air resistance around the shaft, an inflation of 25 layers with a 1.1 growth rate was applied around both of blades and the shaft in order to keep the y^+ values around one. For the current study, the mesh that used in the validation process will be applied to the new geometries as shown in Figure 6.

Table 3. Mesh nodes

Mesh type	Number of the cells
Coarse mesh	32,000
Medium mesh	89,000
Fine mesh	150,000

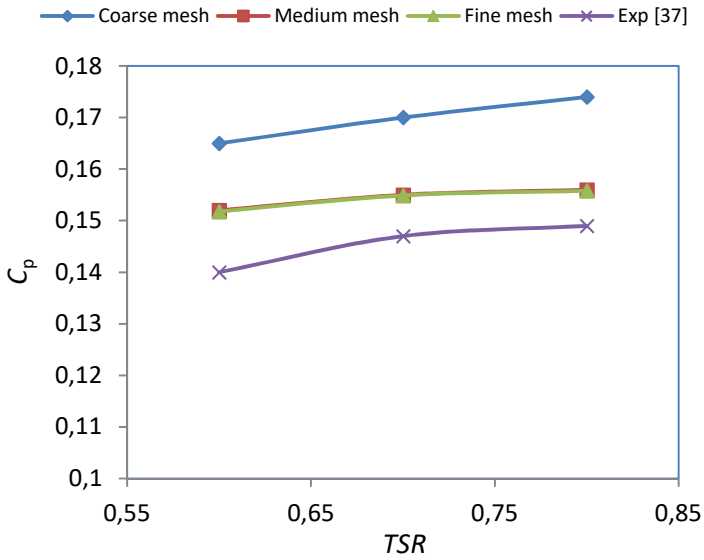

Figure 5. Validation results

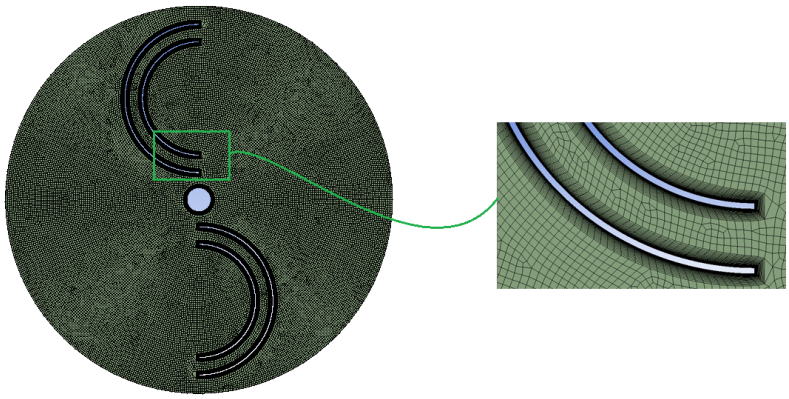

Figure 6. Medium generated mesh

Performance parameters

The performance of wind turbines can be expressed in a dimensionless form. For a certain wind speed, C_p, C_t and *TSR* are effective indicators to evaluate the performance of the turbine. For a particular configuration of Savonius rotor, these parameters are [42]:

$$TSR = \frac{\omega R}{U} \tag{6}$$

$$C_{\mathrm{p}} = \frac{T\omega}{0.5\,\rho A U^3} \tag{7}$$

$$C_{\mathrm{t}} = \frac{T}{0.5\,\rho A R U^2} \tag{8}$$

where R is the radius of the turbine, ω is the angular velocity of the rotor, A is the swept area of the rotor ($A = H \times D$), with H the height of the rotor and T is the average torque.

RESULTS AND DISCUSSION

ANSYS FLUENT 19.2 employed for the simulation purpose, all the experimental data relating to this research were used from Hayashi *et al.* [41] for the validation. Different values of *TSR* (0.4, 0.5, 0.6, and 0.7) were used to determine the C_{p} of the rotor. The results in Figure 5 show that the percentage of error is less than 7% and prove the reliability of the current simulation. From the past few decades, different efficiency enhancement studies on Savonius wind turbines were carried by varying some design parameters such as number of blades and overlap ratio, however, until yet none research has been carried on the effect of the inner blade with various blade arc angles on the rotor. Moreover, previous studies were concluded that the external overlap could reduce the performance of the rotor. On such concept basis, the novel configuration along with an inner blade and external overlap is investigated and compared with the conventional rotor.

Power coefficient comparison

The operation of the Savonius wind rotor depends on the lift and drag forces acting on the blades. Factors like blade angle and blade shape can vary the amount of these forces. Thus, each rotor configuration has its own power coefficient. For that, the C_{p} of the conventional rotor and the novel configuration rotor was investigated and compared. The results were analysed and plotted in Figure 7, where C_{p} is a function of *TSR*.

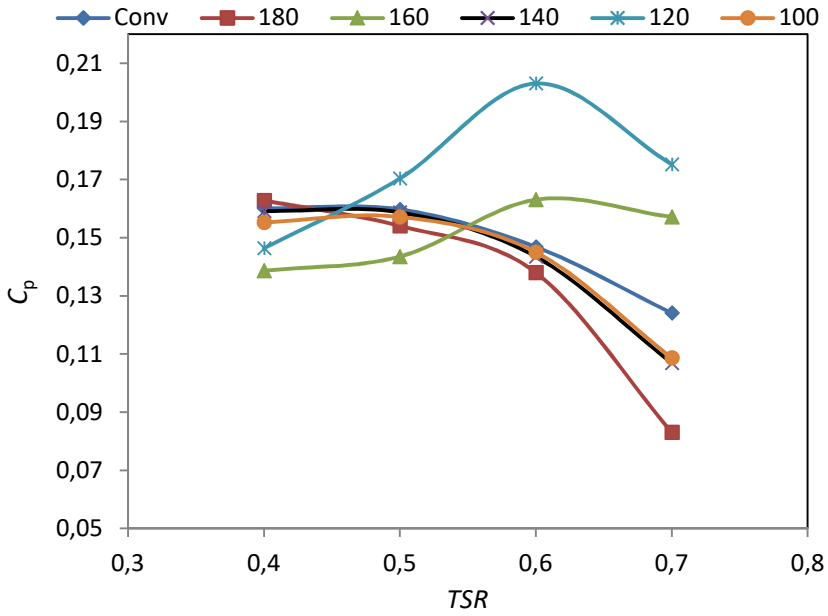

Figure 7. Variations of C_{p} with respect to *TSR*

It can be clearly seen from Figure 7 that model 3 with inner blade arc angle of 120° shows the best performance in terms of C_p followed by model 1 with inner blade angle of 160°. Model 3 at the design points (*TSR* = 0.5, 0.6, 0.7) shows an enhanced percentage of 7%, 39%, 41%, respectively. On the other hand, model 1 shows an improvement of 11% and 26.7% at *TSR* 0.6 and 0.7, respectively. Such enhancements can be related to the pressure drop and rise on the convex and concave side of the rotor respectively. Furthermore, the other models scenarios exhibit slightly lower C_p values than the conventional rotor for most of *TSR* values. Besides, it is also observed that the values of C_p for models 1 and 2 are highly declined at low *TSR* values. Finally, the "main configuration" shows a slightly higher C_p value (2%) than the conventional rotor at *TSR* = 0.4.

Torque coefficient comparison

Figure 8 illustrates the variations of C_t of the conventional and the new simulated configurations at various values of *TSR*s. It can be clearly seen from the figure that the C_t of all simulated rotors including the conventional rotor shows the same trend. Moreover, the configuration with 120° inner blade shows (for most of *TSR* values) higher C_t values than all other simulated rotors. Although the C_t of the new configuration (model 3 with 120° inner blade) is lower at earlier *TSR* value of 0.5, however, C_t increased by a considerable amount at the following values of *TSR*s. This fact indicates that the new model is more effective for high rotational cases. The maximum value of C_t is obtained at 0.4 *TSR* with a value of 0.41, whereas, the lowest value of C_t observed at 0.7 *TSR* for the "main configuration". Generally, for all tested rotors the values of C_t drop with the increase of *TSR*.

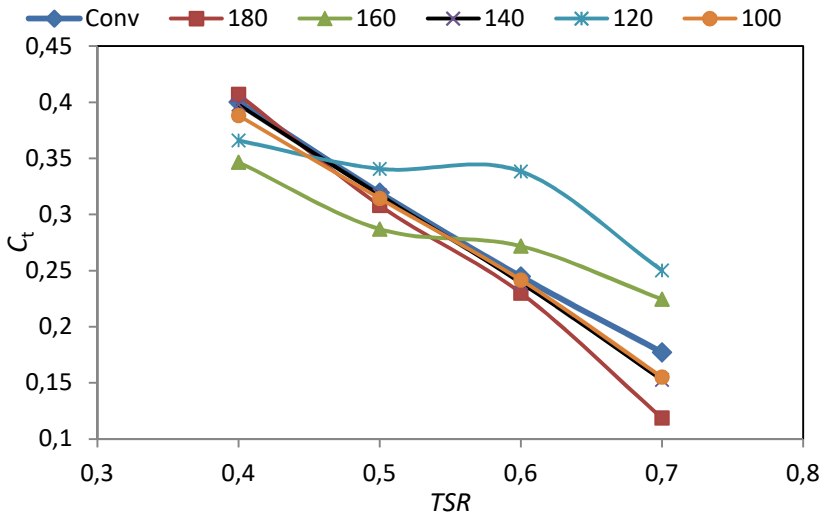

Figure 8. Variations of torque coefficient with respect to *TSR*

The instantaneous C_t at *TSR*s = 0.5 and 0.7 are illustrated in Figure 9 and Figure 10 for all simulated rotors. It is clear that the instantaneous C_t of the rotor with 120° inner blade at *TSR* = 0.5 is increased mostly in the region between 100° and 210° angle of rotation due to the low pressure near the blade tip. Later, this low pressure influences the C_t values to be decreased in the region between 35° and 95°. However, at high considered *TSR* = 0.7, the rotor showed an improvement in terms of C_t at all the regions. Besides, it is also observed from the figures that the maximum torque values were generated close to (90° and 270°) for all configurations at *TSR* = 0.5, and (105°, 290°) for configurations at *TSR* = 0.7. On the other hand, the lowest generated torque occurred around (30° and 180°) at *TSR* = 0.5 and around (20°, 190°) at *TSR* = 0.7. Furthermore, it was observed that at high *TSR* (0.7) the tested rotors experienced negative torque values whereas at low *TSR*

(0.5) all torque values were positive. This difference can be explained due to the amount of pressure reduced outside the blade.

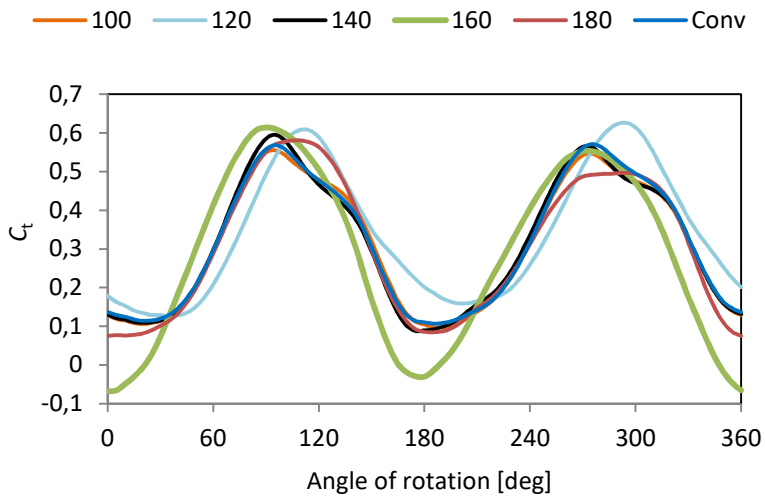

Figure 9. Variation of C_t on the rotor with angle of rotation for $TSR = 0.5$

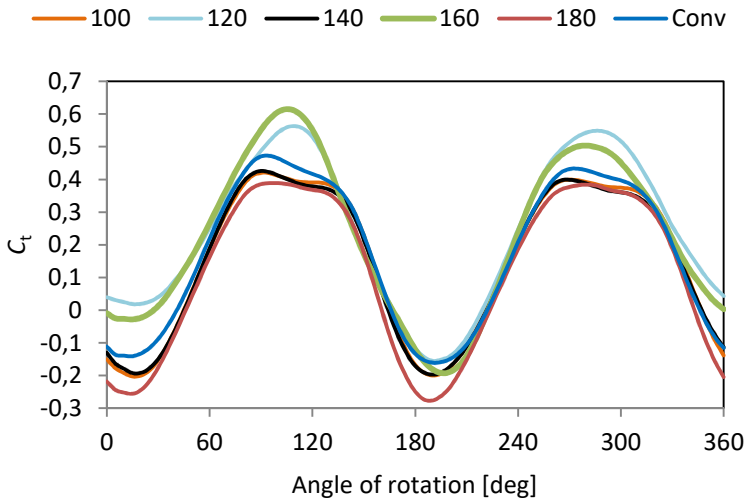

Figure 10. Variation of C_t on the rotor with angle of rotation for $TSR = 0.7$

Velocity and pressure analysis

Pressure and velocity contours for all tested rotors at *TSR* of 0.7 are shown in Figure 11 and Figure 12, respectively. The 9th rotation of the rotor is selected for high accuracy. Angels of rotation (0°, 105°, and 190°) were adopted to analyse the behaviour of pressure and velocity contours. Winds around the rotor start moving with a rotational speed due to the spin of the rotor. This circular motion of the wind contributes to reduce the velocity of the incoming wind on the returning blade which usually affects the performance of the rotor due to the generated resistance between the blade surface and the incoming air. A high-pressure value is noticed on the convex side of the returning blade due to low-velocity around the blade. In contrast, low-pressure zones are much noticed at the tip of the advancing blade which the wind velocity is the maximum. For a better view of the low wind speed zone wind, streamlines are shown in Figure 13. It is clearly shown that the inner blade changed the size and shape of the zone. Savonius rotors spin due to the pressure drag force on the rotors. This force differs with the angle of attack of the blades. Based on that, blades expose their various geometries to the wind stream. Thus, each configuration has its own drag force coefficient. Consequently, the average torque of the rotor changes

with the change of blade position as well as with the rotational speed. Inside the inner blade of the concave side of the returning blade, there is a blue spot which represents a low wind velocity at that point. This may be due to the dragging effects. It is also noticed that the shape of this zone was changed with the change of the blade arc angle. Referring to Figure 11e at $\theta = 0°$ and 190°, high-pressure region is noticed on the convex side of the returning blade more than the other models, and low-pressure region is noticed near the tip of the advancing blade less than the other tested models. This provides evidence that the pressure difference in model 3 is higher than the other models. Thus, the generated torque and power from the rotor in model 3 is higher.

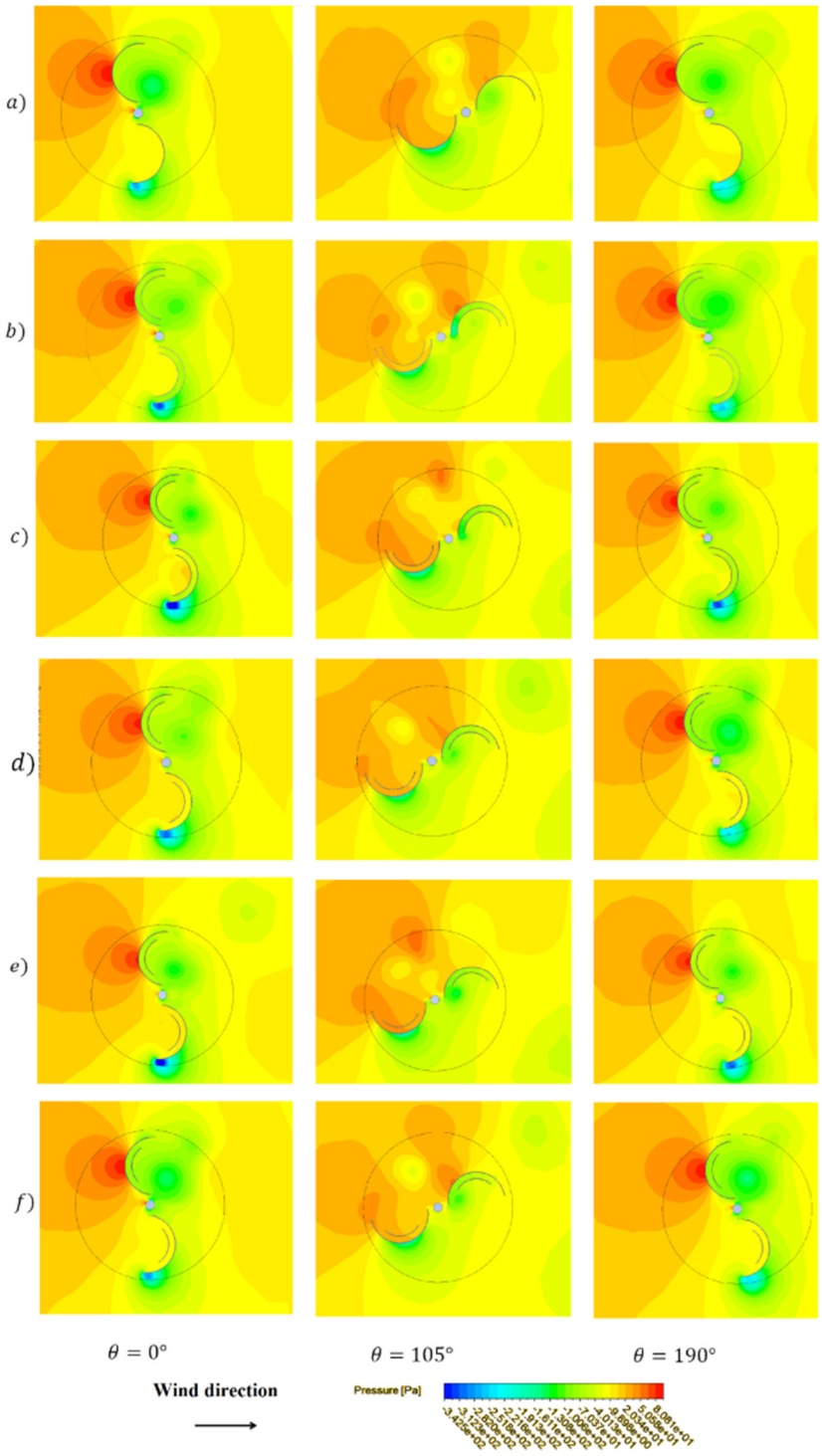

Figure 11. Pressure distribution around blades for: conventional rotor (a); main configuration (b); model 1 (c); model 2 (d); model 3 (e) and model 4 (f)

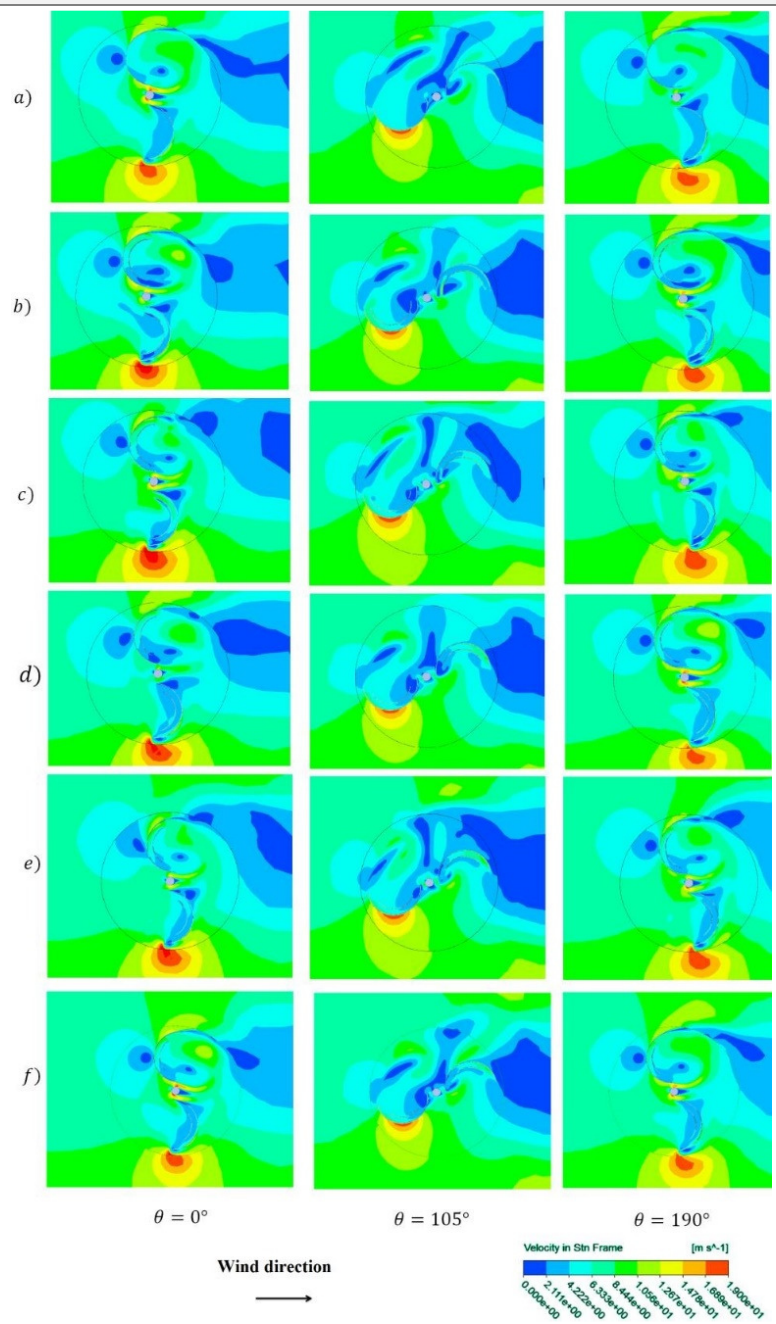

Figure 12. Velocity distribution around blades for: conventional rotor (a), main configuration (b), model 1 (c), model 2 (d), model 3 (e) and model 4 (f)

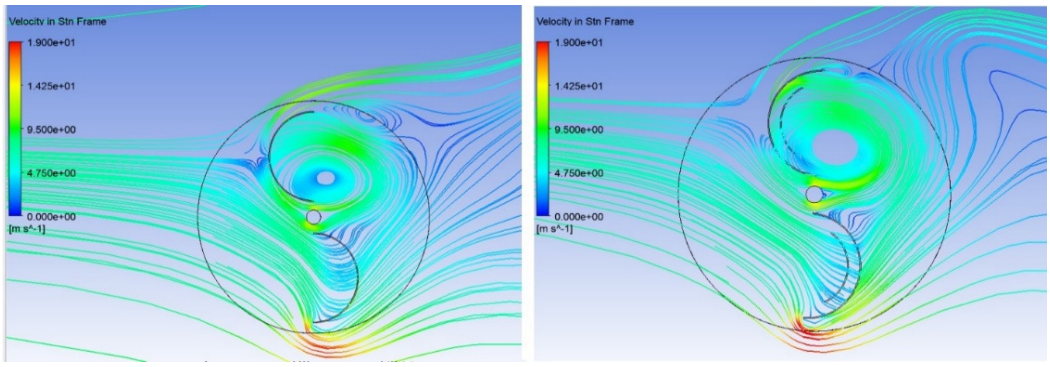

(a) (b)

Figure 13. Streamlines for: conventional rotor (a) and model 3 (b)

CONCLUSIONS

Numerical investigations are performed on five new configurations of Savonius wind rotor with an inner blade, in order to analyze their effect on the rotor efficiency. ANSYS Fluent 19.2 software was utilized to conduct the simulation where the k-ε/Realizable turbulence model was selected. Validation and mesh convergence studies were performed in order to achieve more accurate results. Moreover, y^+ values were controlled during the simulation to be close to 1.

A considerable improvement is noticed with the use of inner blade on the performance of the conventional configuration of Savonius rotor with an external overlap. Maximum C_p improvement was observed to be 41% for inner blade with 120° arc blade angle at $TSR = 0.7$, followed by 39% for the same model at $TSR = 0.6$. On the other hand, inner blade with angle of 140° showed an improvement of 11% and 26.7% at *TSR*s 0.6 and 0.7, respectively. In terms of C_t, it was observed that the main configuration with an inner blade of 180° arc angle showed the maximum value of C_t at *TSR* equal to 0.4 with a value of 0.41 whereas, the lowest value was for the same configuration at *TSR* equal to 0.7.

This new configuration was able to improve the performance of the Savonius rotor at high *TSR* values compared to the conventional rotor. Moreover, it was able to minimize the negative torque on the returning blade at high *TSR*s, which raised the generated torque and so the generated power. Additionally, the inner blade was able to capture the unused portion of the energy of the incoming wind and therefore assisted in enhancing the rotor performance.

Inner blade with a suitable arc angle increases the performance of the Savonius rotor in terms of C_t and C_p without expensive and complex modifications on the geometry. The new configuration (model 3) is more effective for high rotational cases which will introduce a new improvement in the wind machines since the performance of the conventional rotor drops with the increase of *TSR*. Although this new configuration showed a good performance in terms of C_p and C_t, more enhancement in the new configuration could be done by taking into consideration some of the geometrical parameters like solidity factor, inner blade shape, different inner blade design, i.e. aerofoil blades which may improve the performance of the rotor. Future studies can also involve studying the effect of number of inner blades and spacing among blades on the performance of the conventional rotor.

REFERENCES

1. Rea, J. E., Oshman, C. J., Olsen, M. L., Hardin, C. L., Glatzmaier, G. C., Siegel, N. P., Parilla, P. A., Ginley, D. D. and Toberer, E. S., Performance Modeling and Techno-Economic Analysis of a Modular Concentrated Solar Power Tower With Latent Heat Storage, *Appl. Energy*, Vol. 217, pp 143-152, 2018, https://doi.org/10.1016/j.apenergy.2018.02.067
2. Akdağ, S. A. and Güler, Ö., Alternative Moment Method for Wind Energy Potential and Turbine Energy Output Estimation, *Renew. Energy*, Vol. 120, pp 69-77, 2018, https://doi.org/10.1016/j.renene.2017.12.072
3. Marinić-Kragić, I., Vučina, D. and Milas, Z., Concept of Flexible Vertical-Axis Wind Turbine With Numerical Simulation and Shape Optimization, *Energy*, Vol. 167, pp 841-852, 2019, https://doi.org/10.1016/j.energy.2018.11.026
4. Ostos, I., Ruiz, I., Gajic, M., Gómez, W., Bonilla, A. and Collazos, C., A Modified Novel Blade Configuration Proposal for a More Efficient VAWT Using CFD Tools, *Energy Convers. Manag.*, Vol. 180, pp 733-746, 2019, https://doi.org/10.1016/j.enconman.2018.11.025
5. Didane, D. H., Rosly, N., Zulkafli, M. F. and Shamsudin, S. S., Performance Evaluation of a Novel Vertical Axis Wind Turbine With Coaxial Contra-Rotating

Concept, *Renew. Energy*, Vol. 115, pp 353-361, 2018, https://doi.org/10.1016/j.renene.2017.08.070
6. Zhang, B., Song, B., Mao, Z., Tian, W., Li, B. and Li, B., A Novel Parametric Modeling Method and Optimal Design for Savonius Wind Turbines, *Energies*, Vol. 10, No. 3, pp 301, 2017, https://doi.org/10.3390/en10030301
7. Didane, D. H., Rosly, N., Zulkafli, M. F. and Shamsudin, S. S., Numerical Investigation of a Novel Contra-Rotating Vertical Axis Wind Turbine, *Sustain. Energy Technol. Assessments*, Vol. 31, pp 43-53, 2019, https://doi.org/10.1016/j.seta.2018.11.006
8. Sahim, K., Santoso, D. and Puspitasari, D., Investigations on the Effect of Radius Rotor in Combined Darrieus-Savonius Wind Turbine, *Int. J. Rotating Mach.*, Vol. 2018, pp 1-7, 2018, https://doi.org/10.1155/2018/3568542
9. Liang, X., Fu, S., Ou, B., Wu, C., Chao, C. Y. H. and Pi, K., A Computational Study of the Effects of the Radius Ratio and Attachment Angle on the Performance of a Darrieus-Savonius Combined Wind Turbine, *Renew. Energy*, Vol. 113, pp 329-334, 2017, https://doi.org/10.1016/j.renene.2017.04.071
10. ed-Dîn Fertahi, S., Bouhal, T., Rajad, O., Kousksou, T., Arid, A., El Rhafiki, T., Jamil, A. and Benbassou, A., CFD Performance Enhancement of a Low Cut-In Speed Current Vertical Tidal Turbine Through the Nested Hybridization of Savonius and Darrieus, *Energy Convers. Manag.*, Vol. 169, pp 266-278, 2018, https://doi.org/10.1016/j.enconman.2018.05.027
11. Bhuyan, S. and Biswas, A., Investigations on Self-Starting and Performance Characteristics of Simple H and Hybrid H-Savonius Vertical Axis Wind Rotors, *Energy Convers. Manag.*, Vol. 87, pp 859-867, 2014, https://doi.org/10.1016/j.enconman.2014.07.056
12. Ghosh, P., Kamoji, M. A., Kedare, S. P. and Parbhu, S. V., Model Testing of Single- and Three-Stage Modified Savonius Rotors and Viability Study of Modified Savonius Pump Rotor Systems, *International Journal of Green Energy*, Vol. 6, No. 1, pp 22-41, 2009, https://doi.org/10.1080/15435070802701744
13. Al-Ghriybah, M., Çamur, H., Zulkafli, M. F., Khan, M. A., Kassem, Y. and Esenel, E., Study of Multiple Half Blades Effect on the Performance of Savonius Rotor: Experimental Study and Artificial Neural Network (ANN) Model, *Indian J. Sci. Technol.*, Vol. 11, No. 38, pp 1-12, 2018, https://doi.org/10.17485/ijst/2018/v11i38/129966
14. Roy, S. and Saha, U. K., Review on the Numerical Investigations Into the Design and Development of Savonius Wind Rotors, *Renew. Sustain. Energy Rev.*, Vol. 24, pp 73-83, 2013, https://doi.org/10.1016/j.rser.2013.03.060
15. Roy, S. and Saha, U. K., Review of Experimental Investigations Into the Design, Performance and Optimization of the Savonius Rotor, *Proc. Inst. Mech. Eng. Part A: J. Power Energy*, Vol. 227, No. 4, pp 528-542, 2013, https://doi.org/10.1177/0957650913480992
16. Frikha, S., Driss, Z., Ayadi, E., Masmoudi, Z. and Abid, M. S., Numerical and Experimental Characterization of Multi-Stage Savonius Rotors, *Energy*, Vol. 114, pp 382-404, 2016, https://doi.org/10.1016/j.energy.2016.08.017
17. Mahmoud, N. H., El-Haroun, A. A., Wahba, E. and Nasef, M. H., An Experimental Study on Improvement of Savonius Rotor Performance, *Alexandria Eng. J.*, Vol. 51, No. 1, pp 19-25, 2012, https://doi.org/10.1016/j.aej.2012.07.003
18. Worasinchai, S. and Suwannakij, K., Performance Characteristics of the Savonius Turbine, *Proceedings of the IOP Conference Series: Material Science and Engineering*, Vol. 297, Moscow, Russia, April 25-27, 2018, https://doi.org/10.1088/1757-899X/297/1/012056

19. Lin, C.-H. and Klimina, L. A., CFD Simulation and Analysis for Savonius Rotors With Different Blade Configuration, *AIP Conference Proceedings*, Vol. 1637, No. 1, pp 575-581, 2014, https://doi.org/10.1063/1.4904626
20. Kamoji, M. A., Kedare, S. B. and Prabhu, S. V., Experimental Investigations on Single Stage Modified Savonius Rotor, *Appl. Energy*, Vol. 86, No. 7-8, pp 1064-1073, 2009, https://doi.org/10.1016/j.apenergy.2008.09.019
21. Saha, U. K., Thotla, S. and Maity, D., Optimum Design Configuration of Savonius Rotor Through Wind Tunnel Experiments, *J. Wind Eng. Ind. Aerodyn.*, Vol. 96, No. 8-9, pp 1359-1375, 2008, https://doi.org/10.1016/j.jweia.2008.03.005
22. Ahmed, W. U., Zahed, M. J. H., Rahman, M. A. and Mamun, M., Numerical Study of Two and Three Bladed Savonius Wind Turbine, *Proceedings of the 2nd International Conference on Green Energy and Technology*, Vol. 83, pp 36-40, Rome, Italy, 2017, https://doi.org/10.1109/ICGET.2014.6966657
23. Akwa, J. V., Vielmo, H. A. and Petry, A. P., A Review on the Performance of Savonius Wind Turbines, *Renew. Sustain. Energy Rev.*, Vol. 16, No. 5, pp 3054-3064, 2012, https://doi.org/10.1016/j.rser.2012.02.056
24. Ogawa, T., Yoshida, H. and Yokota, Y., Development of Rotational Speed Control Systems for a Savonius-Type Wind Turbine, *J. Fluids Eng.*, Vol. 111, No. 1, pp 6, https://doi.org/10.1115/1.3243598
25. Mohamed, M. H., Janiga, G., Pap, E. and Thévenin, D., Optimization of Savonius Turbines Using an Obstacle Shielding the Returning Blade, *Renew. Energy*, Vol. 35, No. 11, pp 2618-2626, 2010, https://doi.org/10.1016/j.renene.2010.04.007
26. Singh, M. A., Biswas, A. and Misra, R. D., Investigation of Self-Starting and High Rotor Solidity on the Performance of a Three S1210 Blade H-Type Darrieus Rotor, *Renew. Energy*, Vol. 76, pp 381-387, 2015, https://doi.org/10.1016/j.renene.2014.11.027
27. Sutherland, H. J., Berg, D. E. and Ashwill, T. D., A Retrospective of VAWT Technology, Sandia Report No. SAND2012-0304, 2012.
28. Shih, T.-H., Liou, W. W., Shabbir, A., Yang, Z. and Zhu, J., A New k-ϵ Eddy Viscosity Model for High Reynolds Number Turbulent Flows, *Comput. Fluids*, Vol. 24, No. 3, pp 227-238, 1995, https://doi.org/10.1016/0045-7930(94)00032-T
29. Mohamed, M. H., Ali, A. M. and Hafiz, A. A., CFD Analysis for H-Rotor Darrieus Turbine as a Low Speed Wind Energy Converter, *Eng. Sci. Technol. Int. J.*, Vol. 18, No. 1, pp 1-13, 2015, https://doi.org/10.1016/j.jestch.2014.08.002
30. ANSYS I, ANSYS Advantage, 2014, https://www.ansys.com/-/media/ansys/corporate/resourcelibrary/article/ansys-advantage-academic-aa-v8-i1.pdf, [Accessed: 13-June-2019]
31. Abraham, J. P., Plourde, B. D., Mowry, G. S, Minkowycz, W. J. and Sparrow, E. M., Summary of Savonius Wind Turbine Development and Future Applications for Small-Scale Power Generation, *J. Renew. Sustain. Energy*, Vol. 4, No. 4, 042703, 2012, https://doi.org/10.1063/1.4747822
32. Plourde, B. D., Abraham, J. P., Mowry, G. S. and Minkowycz, W. J., Simulations of Three-Dimensional Vertical-Axis Turbines for Communications Applications, *Wind Eng.*, Vol. 36, No. 4, pp 443-453, 2012, https://doi.org/doi:10.1260/0309-524X.36.4.443
33. Fujisawa, N. and Gotoh, F., Pressure Measurements and Flow Visualization Study of a Savonius Rotor, *J. Wind Eng. Ind. Aerodyn.*, Vol. 39, No. 1-3, pp 51-60, 1992, https://doi.org/10.1016/0167-6105(92)90532-F
34. Driss, Z., Damak, A. and Abid, M. S., Evaluation of the Savonius Wind Rotor Performance for Different External Overlap Ratios, *Int. J. Fluid Mech. Therm. Sci.*, Vol. 1, No. 1, pp 14-19, 2015, https://doi.org/10.11648/j.ijfmats.20150101.13

35. Howell, R., Qin, N., Edwards, J. and Durrani, N., Wind Tunnel and Numerical Study of a Small Vertical Axis Wind Turbine, *Renew. Energy*, Vol. 35, No. 2, pp 412-422, 2010, https://doi.org/10.1016/j.renene.2009.07.025
36. Shaheen, M., El-Sayed, M. and Abdallah, S., Numerical Study of Two-Bucket Savonius Wind Turbine Cluster, *J. Wind Eng. Ind. Aerodyn.*, Vol. 137, pp 78-89, 2015, https://doi.org/10.1016/j.jweia.2014.12.002
37. Tian, W., Mao, Z., Zhang, B. and Li, Y., Shape Optimization of a Savonius Wind Rotor With Different Convex and Concave Sides, *Renew. Energy*, Vol. 117, pp 287-299, 2018, https://doi.org/10.1016/j.renene.2017.10.067
38. Mohamed, M. H., Janiga, G., Pap, E. and Thévenin, D., Optimal Blade Shape of a Modified Savonius Turbine Using an Obstacle Shielding the Returning Blade, *Energy Convers. Manag.*, Vol. 52, No. 1, pp 236-242, 2011, https://doi.org/10.1016/j.enconman.2010.06.070
39. Yu, H. and Thé, J., Validation and Optimization of SST K-Ω Turbulence Model for Pollutant Dispersion Within a Building Array, *Atmos. Environ.*, Vol. 145, pp 225-238, 2016, https://doi.org/10.1016/j.atmosenv.2016.09.043
40. Sharma, S. and Sharma, R. K., Performance Improvement of Savonius Rotor Using Multiple Quarter Blades – A CFD Investigation, *Energy Convers. Manag.*, Vol. 127, pp 43-54, 2016, https://doi.org/10.1016/j.enconman.2016.08.087
41. Hayashi, T., Li, Y. and Hara, Y., Wind Tunnel Tests on a Different Phase Three-Stage Savonius Rotor, *JSME Int. J. Ser. B*, Vol. 48, No. 1, pp 9-16, 2005, https://doi.org/10.1299/jsmeb.48.9
42. Kerikous, E. and Thévenin, D., Optimal Shape of Thick Blades for a Hydraulic Savonius Turbine, *Renew. Energy.*, Vol. 134, pp 629-638, 2019, https://doi.org/10.1016/j.renene.2018.11.037

Paper submitted: 08.03.2019
Paper revised: 24.04.2019
Paper accepted: 30.04.2019